Analytical and numerical modelling of a buckling in a plastic regime of a homogeneous console with symmetrical cross section

© V.V. Chistyakov

Ioffe Institute,
194021 St. Petersburg, Russia
e-mail: v.chistyakov@mail.ioffe.ru

The method of numerical-analytical modeling using Maple 18 of the strong buckling of a uniform console with a symmetrical cross-section is presented. The range of plastic deformations in a materials with conditional yield strength (CYS) is studied. Standard profiles and sections made of low-carbon steel, titanium, polyethylene etc. were investigated. Were found and compared with the proper Eulerian values the critical loads of F_{cr}, N, the shape of buckled console $y(z)$. The quasi-identity of the latter is established for the same slope $p_f = dy/dz$ near the free console end. The method can be applied in robotics, structural mechanics, medical prosthetics, etc. where the materials been used with relatively high Young's modulus and low the CYS.

Keywords: buckling, plastic deformations, conditional yield strength, critical load, Maple.

DOI: 10.61011/TP.2023.12.57715.f207-23

Euler's problem of buckling of a beam/column/console under longitudinal load in the range of inelastic strains of the material is relevant in many industries, such as sports (pole vaulting), construction (bridges and truss structures), robotics, medical prosthetics, etc. Therefore, starting with the research of F.R. Shanley [1], it has attracted a large number of researchers — from structural strength engineers to pure mathematicians studying bifurcations, as well as nanotechnologists synthesizing materials based on carbon nanotubes [2].

For a number of metals with a high so-called offset yield strength (OYS), the plastic mode is relevant in the case of short consoles (stubs), when it is necessary to consider the resulting shear deformations that take the problem out of the category of one-dimensional [3–5]. However, for the increasingly widely used polymers with high Young's modulus but low OYS (Teflon [6], high-density polyethylene HDPE, etc.), the plasticity can be considered in the scope of the plane-sections hypothesis (PSH), which is the topic of this paper.

The author aspired to simplify the computational part of the problem as much as possible through analytical transformations and the use of model representations that significantly reduce this part. These include:

a) cubic formula for the strain-stress diagram of the material with the presence of the OYS and the densification zone;

b) symmetry of the console cross-section.

A homogeneous console AB of free length (l_0) and a cross-section (S) symmetrical with respect to the axis x of buckling is considered. The lower end A is rigidly clamped, while to the upper B is applied a distributed across the section compressive axial load F (Fig. 1, a).

According to the PSH, the relative deformation in the cross-section layer with the internal coordinate η (Fig. 1, b) is determined by the expression $\varepsilon_\eta = \varepsilon_{ax} + \frac{\eta}{\rho}$, where $\rho(z)$ and ε_{ax} — are the radius of curvature of the axis and its strain in the cross-section with the vertical coordinate z.

Then, in the assumption of a cubic compressive diagram (see below), the stress can be represented by a series of

$$\sigma(\varepsilon) = \sigma(\varepsilon_{ax}) + \frac{d\sigma(\varepsilon_{ax})}{d\varepsilon}\frac{\eta}{\rho} + \frac{1}{2!}\frac{d^2\sigma(\varepsilon_{ax})}{d\varepsilon^2}\left(\frac{\eta}{\rho}\right)^2$$
$$+ \frac{1}{3!}\frac{d^3\sigma(\varepsilon_{ax})}{d\varepsilon^3}\left(\frac{\eta}{\rho}\right)^3,$$

and the bending moment in the cross-section z is defined as

$$M_z(z) = \iint \sigma_z \eta \, dS = \frac{d\sigma(\varepsilon_{ax})}{d\varepsilon}\frac{J_x^{(II)}}{d\varepsilon} + \frac{1}{3!}\frac{d^3\sigma(\varepsilon_{ax})}{d\varepsilon^3}\frac{J_x^{(IV)}}{\rho^3}$$

with $J_x^{(II)}$ and $J_x^{(IV)}$ — area moments II and IV orders (the term with $J_x^{(III)} = 0$ disappears).

Substituting $1/\rho = y'_{zz}/(1 + y'^2_z)^{\frac{3}{2}}$, we get the governing equation of buckling

$$\frac{d\sigma(\varepsilon_{ax})}{d\varepsilon}\frac{J_x^{(II)}y''_{zz}}{(1 + y'^2_z)^{\frac{3}{2}}} + \frac{1}{6}\frac{d^3\sigma(\varepsilon_{ax})}{d\varepsilon^3}\frac{J_x^{(IV)}(y_{zz})'^3}{(1 + y'^2_z)^{\frac{9}{2}}}$$
$$= -(F_y + M_A), \tag{1}$$

where $M_A = -Fb$ — the embedding torque A and the value b — the lateral displacement of the upper end B. By substituting $v = y = b$, $v' = p$ $\left(pv'_{zz} = p\frac{dp}{dv} = v\frac{dp^2}{dv^2}\right)$ and
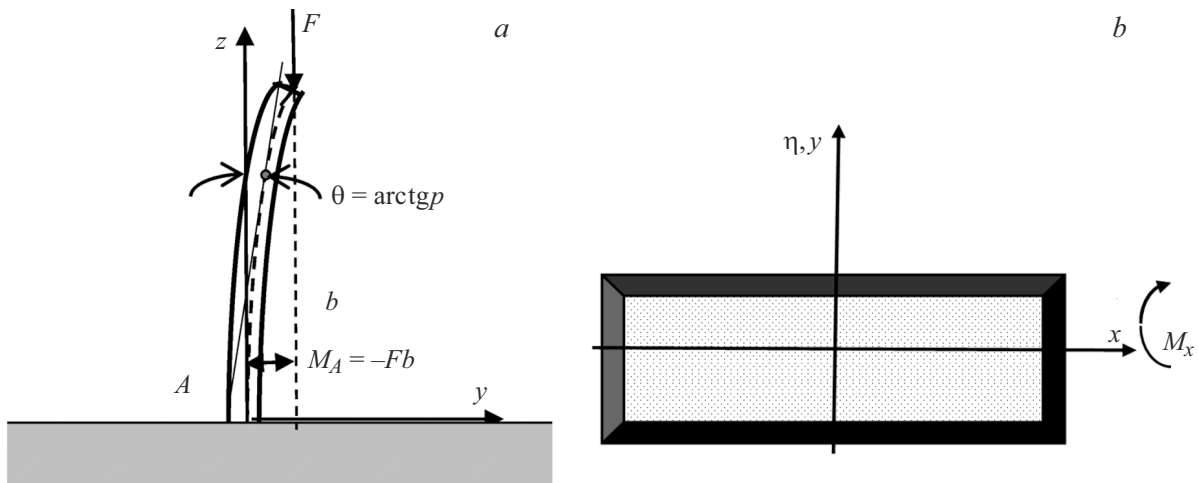
Figure 1. *a* — console with lower end fixed *A* and loaded top *B* and symmetrical cross-section (*b*) with zero odd area moments $J_x^{(2n+1)} = 0$.

$v^2 \equiv w$, $p^2 \equiv s$ we get

$$
\begin{cases}
\frac{dw}{ds} = -\frac{J_x^{(II)}}{F(1+s)^{\frac{3}{2}}} \left(\frac{d\sigma(\varepsilon_{ax})}{d\varepsilon} \right) - \frac{1}{6} \left(\frac{d^3\sigma(\varepsilon_{ax})}{d\varepsilon^3} \right) \frac{J_x^{(IV)} w}{F(1+\varepsilon)^{\frac{9}{2}} \left(\frac{dw}{ds} \right)^2}, \\
w(0) = b^2, \quad w(p_f^2) = 0, \quad p_f = \frac{dy(z_B)}{dz}, \\
\sigma_{ax}(p) = \frac{F\cos\theta}{S} = \frac{F}{S(1+s)^{\frac{1}{2}}}.
\end{cases} \tag{2}
$$

A simple cubic formula for a compression diagram,

$$
\sigma(\varepsilon) = E\varepsilon - \frac{3E\mu}{2}\varepsilon^2 + \frac{E\mu}{2t}\varepsilon^3, \qquad \mu = \frac{Et - \sigma_f}{Et^2},
$$

$$
\sigma_f - \text{OYS}, \qquad t = \varepsilon(\sigma_f), \tag{3}
$$

the derivatives of which

$$
\frac{d\sigma(\varepsilon)}{d\varepsilon} = E - 3E\mu\varepsilon + \frac{3E\mu}{2t}\varepsilon^2, \quad \frac{d^3\sigma(\varepsilon)}{d\varepsilon^3} = \frac{3\mu E}{t} \tag{4}
$$

and the inverse to it (also cubic, but without a densification zone)

$$
\varepsilon(\sigma) = \frac{\sigma}{E} + \frac{3\mu\sigma^2}{2E^2} + \frac{\mu(9\mu t - 1)\sigma^3}{2E^3 t} \tag{5}
$$

well describe the compression of Teflon, HDPE, steel (Fig. 2), and other materials.

The substitution (5) to (4) gives an approximation in a third order of the value σ:

$$
\frac{d\sigma}{d\varepsilon}(\sigma) = E - 3\mu\sigma + \left(\frac{3\mu}{2Et} - \frac{9\mu^2}{2E} \right)\sigma^2 + \left(\frac{6\mu^2}{E^2 t} - \frac{27\mu^3}{2E^2} \right)\sigma^3.
$$

Navigating to the variables $w = v^2$ *vs* $s = p^2$ converts the equation to the form

$$
\frac{dw}{ds} = -\frac{J_x^{(II)}}{F(1+s)^{3/2}} + \frac{eJ_x^{(II)}\mu}{S(1+s)} - \frac{J_x^{(II)}\left(\frac{3\mu}{2Et} - \frac{9\mu^2}{2E} \right)}{S^2(1+s)^{5/2}}F
$$

$$
-\frac{J_x^{(II)}\left(\frac{6\mu^2}{E^2 t} - \frac{27\mu^3}{2E^2} \right)}{S^3(1+s)^3}F^2 - \frac{\mu E}{2t} \frac{J_x^{(IV)} w}{F(1+s)^{\frac{9}{2}} \left(\frac{dW}{ds} \right)^2}, \tag{6}
$$

which in a zero approximation of the small value $J_x^{(IV)}$ has a solution

$$
w_0(s) = \frac{2J_x^{(II)}}{F(1+s)^{1/2}} - \frac{3J_x^{(II)}\mu}{S(1+s)^2} + \frac{2J_x^{(II)}\left(\frac{3\mu}{2Et} - \frac{9\mu^2}{2E} \right)}{3S^2(1+s)^{5/2}}F
$$

$$
+ \frac{J_x^{(II)}\left(\frac{6\mu^2}{E^2 t} - \frac{27\mu^3}{2E^2} \right)}{S^3(1+s)^3}F^2 - \left(\frac{2J_x^{(II)}}{F(1+p_f^2)^{1/2}} - \frac{3J_x^{(II)}\mu}{S(1+p_f^2)} \right.
$$

$$
+ \frac{2J_x^{(II)}\left(\frac{3\mu}{2Et} - \frac{9\mu^2}{2E} \right)}{3S^2(1+p_f^2)^{5/2}}F + \left. \frac{J_x^{(II)}\left(\frac{6\mu^2}{E^2 t} - \frac{27\mu^3}{2E^2} \right)}{2S^3(1+p_f^2)^3}F^2 \right). \tag{7}
$$

The transverse coordinate is determined as

$$
y(p) = v_0(p) + b = b - \sqrt{w_0(p^2)},
$$

the longitudinal coordinate — $z(p) = \int_0^p \frac{dv_0(p')}{p'}$, and the axis length element — $dl(p) = \frac{dv_0(p)\sqrt{1+p^2}}{p} = -\frac{dw_0}{ds}\sqrt{\frac{1+p^2}{w_0}}$.
Restored length element $dl_{res}(p) = \frac{dl(p)}{1-\varepsilon(p)} \approx \frac{dw_0}{dp^2}\sqrt{\frac{1+p^2}{w_0}} \times$
$\times \left(1 + \varepsilon(p) + \varepsilon^2(p) + \varepsilon^3(p) \right)$: the recovered axis length itself (l_0)

$$
-\int_0^{p_f} \frac{dw_0}{dp^2} \frac{\sqrt{1+p^2}}{\sqrt{w_0}}(1+\varepsilon(p)) + \varepsilon^2(p) + \varepsilon^3(p))dp
$$

$$
= L(F, p_f) = l_0. \tag{8}
$$

This relation defines the dependence of the final slope on the load $p_f(F)$ (Fig. 3, *a*). For consoles made of HDPE plastics, the slenderness of $\lambda = l_0\sqrt{\frac{S}{J^{(II)}}} \sim 10 - 15$ is close to $\sigma_f = 26$ MPa. There is an approximately 40% drop in the critical load F_{cr} compared to Euler's formula for the
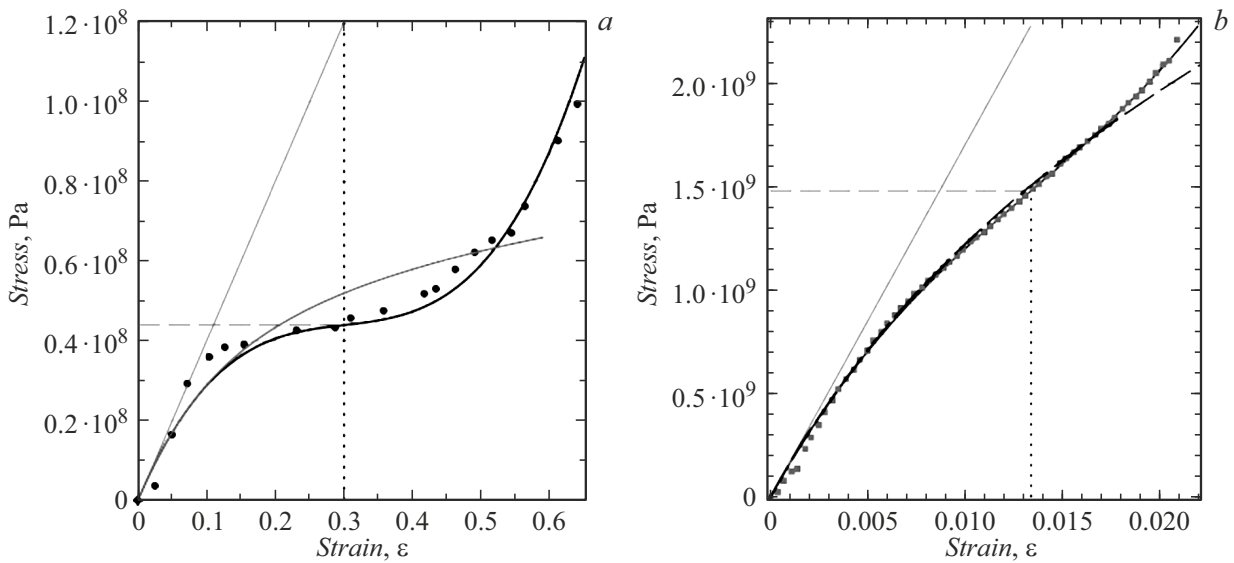
Figure 2. Compressive strain-stress diagrams: a — Al/PTFE: experiment [6] (circles), cubic model $\sigma(\varepsilon)$ (3) with $E = 400$ MPa, $\sigma_f = 44$ MPa, $t = 0.3$, $E_{\text{tang}} = 55.8$ MPa (solid black curve), Hooke's law (continuous narrow gray line), inverse diagram $\varepsilon(\sigma)$ (continuous wide gray curve), yield strain (black dots), yield stress (gray strokes); b — steel: diamonds — experimental points, solid black curve — model $\sigma(\varepsilon)$ (3) with parameters $E = 170$,GPa, $\sigma_f = 1.48$ GPa, $t = 0.0134$, solid gray line — Hooke's law, dashed black curve — inverse relationship $\varepsilon(\sigma)$ (5), gray strokes — stress σ_f, black dots — strain t.
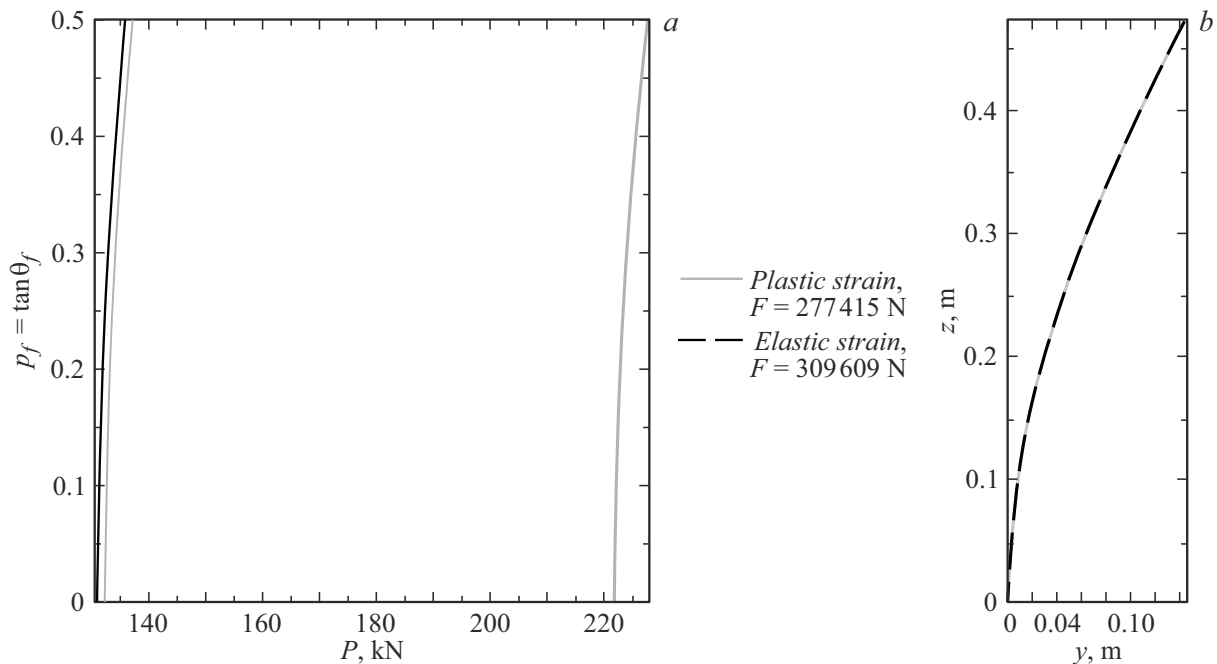

Figure 3. a — dependency for rectangular-tubular HDPE console (Fig. 1) $S = 0.0102$ m^2, $J^{(\mathrm{II})} = 4.5 \cdot 10^{-5}$ m^4, $l_0 = 0.75$ m: gray wide curve — Hooke's law with $E = 1.08$ GPa; black curve — diagram (3) with $t = 0.05$, $\sigma_f = 26$ MPa; gray narrow curve — approximation of the tangent module; b — complete identical shape of the console (steel I-beam № 10, $l_0 = 0.5$ m) at $p_f = 0.5$ for the case of Hooke's Law (long black strokes, 309 kN) and diagram (3) (gray continuous curve, 277 kN).

elastic case. The tangent modulus approximation [1] gives a result close in the value F_{cr} to that resulting from the cubic formula 3), but slightly exceeding it.

Applying the formulas for coordinates y and z, we obtain the buckling shapes of the console of a given length at a given upper end slope p_f within various approximations, namely for Hooke's law and a cubic

diagram (3) (Fig. 3, *b*). It is observed almost identical buckling shape for the same value p_f within different approximations.

Conflict of interest

The author declares that he has no conflict of interest.

References

[1] F.R. Shanley. J. Aeronautical Sci., **14** (5), 261 (1947).
[2] S. Gupta, S. Pramanik, S. Smita, S.K. Das, Sh. Saha. Wave Motion, **104** (1),102730 (2021).
DOI: 10.1016/j.wavemoti.2021.102730
[3] A. Afroz, T. Fukui, in book: *Bifurcation and Buckling Structures* (CRC Press, Boca Raton, 2021), p. 12.
DOI: 10.1201/9781003112365
[4] Sh. Fan, D. Dong, T. Zhu, J. Wang, W, Hou. J. Constructional Steel Research, **198** (2), 107516 (2022).
DOI: 10.1016/j.jcsr.2022.107516
[5] S.P. Timoshenko, J.M. Gere. *Theory of Elastic Stability* (McGraw-Hill book company, NY., USA, 1961)
[6] Ch. Chen, Z. Guo, E. Tang. Polymers, **15**, 702 (2023).
DOI: 10.3390/polym15030702

Translated by 123